Laser Photolysis of TiO_2 Layers in the Presence of Aqueous Iodide

David Behar

Soreq Nuclear Research Center, Yavne 81800, Israel

Joseph Rabani*

Department of Physical Chemistry and the Farkas Center, The Hebrew University of Jerusalem, Jerusalem 91904, Israel

Received: September 5, 2000; In Final Form: April 11, 2001

Laser photolysis of TiO_2 porous layers has been studied using iodide as a hole-scavenger. The I_2^- transient product, which is produced inside the layer, decays predominantly by the second-order reaction with TiO_2 electrons and by disproportionation. The resulting I_3^- ion also reacts with the TiO_2 electron, although the rate of reaction is 2 orders of magnitude slower than I_2^-. Evaluation of the rate constants was achieved by fitting computed curves of absorbance vs time profiles to the experimental data. The rate constants $k(e^-_{TiO2} + I_2^-) = (2.25 \pm 0.6) \times 10^5$, $k(e^-_{TiO2} + I_3^-) = (1.65 \pm 0.4) \times 10^3$, and $k(I_2^- + I_2^-) = (1.1 \pm 0.15) \times 10^5\ M^{-1}\ s^{-1}$ have been determined in the TiO_2 layer. The rate constants suggest relatively low diffusion rates for I_2^- radical ion and e^-_{TiO2}. These have been attributed to electron trapping at nanocrystallite boundaries as well as activation and steric barriers. The rate of reaction of I_3^- with the TiO_2 electron suggests that this reaction must be important in photoelectrochemical cells involving iodide and iodine. The high photocurrent yields observed in some of these cells, is attributed to dense coverage of the TiO_2 surface by the photosensitizer.

Introduction

The detailed mechanism of reactions involving illuminated TiO_2 is of major importance for applications of photocatalytic mineralization of pollutants[1−4] and dye sensitized photoelectrochemical solar cells.[5−7] The latter are mostly based on TiO_2 layer and iodide/iodine charge carrier. The main mechanistic difference between the initial step of the photocatalytic and photoelectrochemical processes is the nature of the TiO_2 hole. In almost all the photocatalytic systems, the excitation light is absorbed directly by the TiO_2 nanocrystallites yielding charge separation according to reaction 1. On the other hand, photosensitization involves electron injection from the excited state of the photosensitizer to the conduction band of the TiO_2. The hole, in the form of oxidized photosensitizer remains at the surface.

The primary step in the photocatalytic reaction mechanism is the generation of pairs of electrons and holes in the TiO_2 particles (reaction 1), where h_{VB}^+ stands for valence band holes and e_{CB}^- represents conduction band electrons. The possibility of electron and hole trapping (reactions 2−3) has been discussed previously.[8−25]

$$TiO_2 \xrightarrow{h\nu} h_{VB}^+ + e_{CB}^- \quad (1)$$

$$e_{CB}^- \rightarrow e_{tr}^- \quad (2)$$

$$h_{VB}^+ \rightarrow h_{tr}^+ \quad (3)$$

At high laser intensities, where several electron−hole pairs are produced per nanocrystallite, most of the absorption decays within less than 1 ns according to reaction 4.[26] On the other hand, when an average of less than one electron−hole pair per nanocrystallite is present, decay of absorbance can be observed in the ns-μs time range. These decays have been attributed to reaction of trapped electrons with mobile or trapped holes, as described by reaction 5 and 6,[9−11,27] although ns measurements

$$e_{CB}^- + h_{VB}^+ \rightarrow TiO_2 \quad (4)$$

$$e_{tr}^- + h_{VB}^+ \rightarrow TiO_2 \quad (5)$$

$$e_{tr}^- + h_{tr}^+ \rightarrow TiO_2 \quad (6)$$

of spectral changes in the presence of high iodide concentration have been recently attributed to electron migration to lower traps.[24]

It has been shown that different methods of preparation of TiO_2 may induce different behavior under otherwise identical conditions.[10,15,28] This might introduce uncertainty when a unifying interpretation is based on results of different preparations.

Considerable work has been carried out with iodide ions, mostly in colloid solutions.[16,24,29−33] Henglein,[16] Grabner and Quint,[30] Moser and Graetzel,[31] and Rabani et al.[24] studied quantum yields of iodide oxidation by the TiO_2 hole under various conditions. Fitzmaurice, Frei, and their co-workers[32,33] investigated the kinetic behavior of I_2^- in photosensitized TiO_2 sols. In view of the special importance of the TiO_2−iodide/iodine couple, we carried out mechanistic studies on the TiO_2−iodide system in the form of nanocrystallite layers using laser photolysis, extending the kinetic studies up to the range of several seconds.

Experimental Section

Preparation of the TiO_2 Layers. Thin layers of TiO_2 on ITO/glass, were prepared by 15 successive spin coatings of

* To whom correspondence should be addressed. E-mail: rabani@vms.huji.ac.il

10.1021/jp003176w CCC: $20.00
Published on Web 06/16/2001

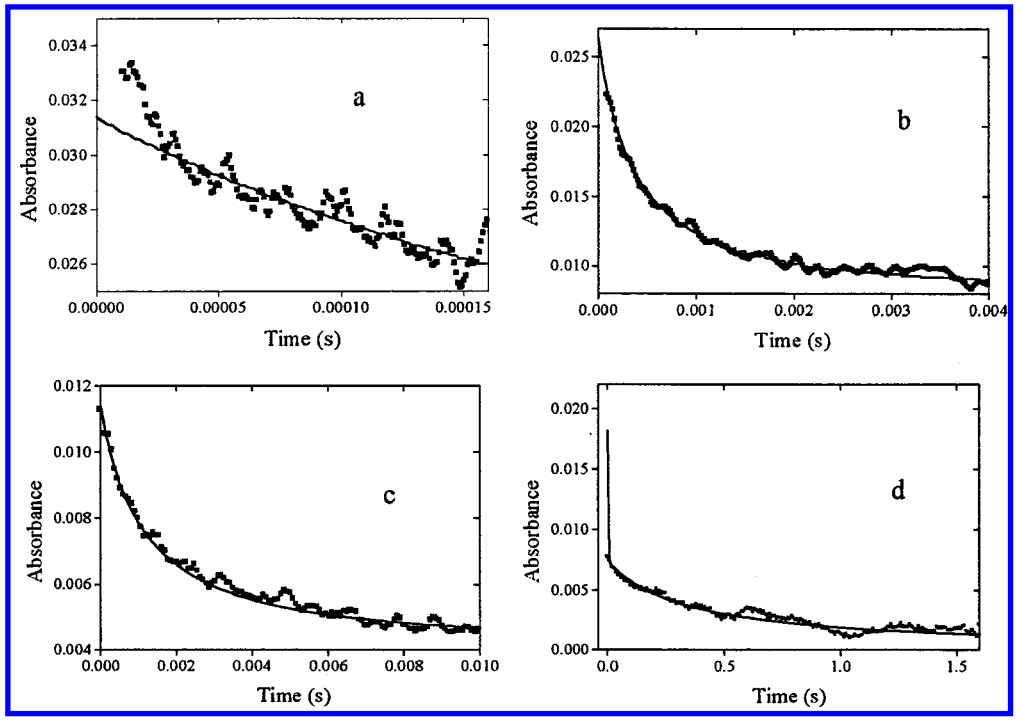

Figure 1. Decay of the 390 nm absorbance. Time profile following laser pulse illumination of TiO_2 layer in "Sandwich" configuration, Ar saturated 7.3 M NaI. Laser intensity (2.3×10^{-8} ein cm^{-2} per pulse). Solid lines: computer simulations using $k_{10} = 1.05 \times 10^5$, $k_{11} = 1.63 \times 10^3$ M^{-1} s^{-1}, and $\epsilon_{12-} = 11\,400$, $\epsilon_{13-} = 23\,300$ M^{-1} cm^{-1}. (a) $[e^-_{TiO2}]_0 = [I_2^-]_0 = 9.3$ mM, $k_9 = 1.66 \times 10^5$ M^{-1} s^{-1}. (b) $[e^-_{TiO2}]_0 = [I_2^-]_0 = 7.7$ mM, $k_9 = 2.6 \times 10^5$ M^{-1} s^{-1}. (c) $[e^-_{TiO2}]_0 = [I_2^-]_0 = 3.3$ mM, $k_9 = 1.8 \times 10^5$ M^{-1} s^{-1}. (d) $[e^-_{TiO2}]_0 = [I_2^-]_0 = 5.3$ mM, $k_9 = 1.8 \times 10^5$ M^{-1} s^{-1}.

colloidal TiO_2 solutions (1 min at 3500 rpm) yielding 3 μm thickness with D_{355} 1.0−1.2. The TiO_2 layers showed much better mechanical stability than TiO_2 layers on glass. TiO_2 colloid solutions were prepared by hydrolysis of titanium 2-propoxide (Aldrich) at near 0 °C according to the reported procedure,[34] yielding particles with average diameter of 4 nm. Solutions containing 200 g/L TiO_2 (D_{355} of a 1/1000 solution was 0.13) at pH 2.5 (HNO_3) were used for spin coating. The ITO/glass plate carrying the TiO_2 layers, with the dimensions 0.9×2.5 cm^2, was coupled with a bare plate of similar dimensions. The two plates where separated by a thin spacer (50 μm thickness) and tightly held together by means of an appropriate slit at a Teflon base at the bottom of a four windows glass cell. A specially fitted cover held the two plates tightly together at the top. The cell was flushed with Ar gas for at least 20 min prior to photolysis. Air free NaI solution (200 μL, typical concentration 7 M) was injected through a rubber septum. The solution filled the space between the plates due to capillary forces.

Laser Illuminations. Kinetic measurements and transient spectra were carried out using Nd:YAG laser pulses (Product of J K Lasers, 12 ns half-width) at 355 nm, with 5 mJ/pulse. The laser excitation beam, 7 mm diameter, entered the samples at 90° to the analytical light hitting first the glass support of the ITO/TiO_2 layer at an angle of 45°. The analytical light source was a 75-W xenon lamp. Whenever required, a voltage pulse of several ms was applied in order to achieve 40-folds increase of the light intensity. The light signals were analyzed with the aid of Hamamatsu R928 photomultiplier, B&L monochromator and Tektronix TDS 620B digitizer. The analytical light reaching the layer passed through 2 mm diameter pinhole located at the bare ITO/glass at the center of the laser beam, to ensure complete overlap between the laser and analytical lights. Laser light intensities were attenuated with the aid of appropriate glass filters.

Kinetic data processing was carried out using a computer program for solving simultaneous kinetic equations, generously provided by Dr. Herold A. Schwarz of Brookhaven National Laboratory

Results and Discussion

Measurements at 390 nm. Upon applying a 355 nm laser pulse on TiO_2 layer immersed in concentrated iodide solution, a pronounced absorbance change at 390 nm is produced. This absorption, due to formation of the I_2^- ion radical, is fully developed at the end of the 12 ns pulse according to reactions 7 and 8

$$h^+ + I^- \rightarrow I \quad (7)$$

$$I + I^- \rightarrow I_2^- \quad (8)$$

The quantum yield of I_2^- was measured from its initial extrapolated absorbance produced by laser pulse intensity of 1.2×10^{-9} ein cm^{-2} per pulse. $\Delta D^{390} = 0.0069$ (average of 128 pulses), corresponding to a quantum yield $\varphi(I_2^-) = 0.9$. This value is based on actinometry with $Ru(bpy)_3^{2+}$ at 480 nm, $\Delta\epsilon = \epsilon(Ru(bpy)_3^{2+}) - \epsilon(Ru(bpy)_3^{2+})^* = 3.64 \times 10^3$ M^{-1} cm^{-1},[35] and $\epsilon_{I2^-}{}^{390} = 1.14 \times 10^4$ M^{-1} cm^{-1}.

The decay of absorption at 390 nm is attributed to reactions 9−11

$$I_2^- + e^-_{TiO2} \rightarrow 2I^- \quad (9)$$

$$I_2^- + I_2^- \rightarrow I_3^- + I^- \quad (10)$$

$$I_3^- + e^-_{TiO2} \rightarrow I_2^- + I^- \quad (11)$$

Figure 1 shows typical absorbance vs time profiles together with simulated curves based on the second-order reactions 9−11 at

different time ranges. The simulated results fit very well with the experiments in the time range from 30 μs to 1.6 s. A faster decay is observed during the first 30 μs (see later). Average values for best fits of 20 traces such as shown in Figure 1 are $k_9 = (2.25 \pm 0.6) \times 10^5$, $k_{10} = (1.1 \pm 0.15) \times 10^5$, and $k_{11} = (1.65 \pm 0.4) \times 10^3$ M^{-1} s^{-1}. These average values are best fits for the entire time range up to at least 1.6 s. The extinction coeffs $\epsilon_{I3^-}^{390} = 2.33 \times 10^4$ and $\epsilon_{I2^-}^{390} = 1.14 \times 10^4$ M^{-1} cm^{-1} were used for the computations. The value of $\epsilon_{I3^-}^{390}$ strongly depends on iodide concentration. The above value, applying to 7 M NaI, was determined in the present work. It is much higher than the literature one ($\epsilon_{I3^-}^{390} = 9300$ M^{-1} cm^{-1} for dilute iodide solution).[36] Pulse radiolytic measurements were carried out providing a value $\epsilon_{I2^-}^{390} = (1.14 \pm 0.05) \times 10^4$ M^{-1} cm^{-1}, independent of iodide concentration in the range 0.01−7 M. This value is 22% higher than previously reported.[37]

The second order nature of the decay indicates that the initially produced I_2^- and e^-_{TiO2} no longer exist as pairs, and the microvolume where the reactions take place is composed of a number of nanocrystallites, containing a large number of radicals. Had reaction 9 involved the initial $I_2^- - e^-_{TiO2}$ pairs, an apparent first-order rate law, or a multiexponential decay would have been observed. A multiexponential decay has been suggested in layer systems and assigned to distance distribution.[38,39] The good fit of the simulations based on the second-order reactions 9−11 to the experimental results in the time range from 30 μs to 1.5 s, and 3-fold variation of initial radical concentration is not in favor of a single or multiexponential assignment of the decay. It should be noted that the simulated traces are very sensitive to the values of the rate constants. Although three reactions are involved, reaction 11 is fairly well separated in time from reactions 9 and 10. In addition, reaction 9 involves decay while reaction 11, has hardly any effect on the absorbance since $\epsilon_{I3^-} \approx 2\epsilon_{I2^-}$. Therefore, the level of the near plateau absorbance (Figure 1) is very sensitive to the ratio k_9/k_{10}, whereas the rate of the decay to this near plateau value is sensitive to the absolute values of these rate constants. In view of this, the accuracy of the reaction rate constants derived from the results of the simulations is similar to that in calculating reaction rates of simple reactions.

The decay of absorbance is faster in the first 30 μs (see the initial part of the decay in Figure 1a). During $t < 8$ μs, a rough fit can be obtained yielding an average value $k_{9\sim1.5} \times 10^6$ M^{-1} s^{-1}, which gradually decreases with time. This observation is attributed to time dependency of k_9, which is expected to take place as long as the distance between e^-_{TiO2} and I_2^- produced at the same nanocrystallite is considerably smaller than the average distance between reactants from different pairs. A simple calculation based on $\epsilon_{I2^-} = 1.14 \times 10^4$ M^{-1} cm^{-1}, 2 nm radius of the average nanocrystallite (as measured by electron microscopy) and 3 μm layer thickness, shows that at high laser pulse intensities, producing $D_0^{390} = 0.03$, the ratio of TiO_2 nanocrystallites to $e^-_{TiO_2} - I_2^-$ pairs initially produced is ~4.

Inhomogeneous Light Absorption across the TiO_2 Layer. With average absorbance of 1.1, the excitation light decreases rapidly across the TiO_2 layer. Thus, it can be shown that the intensity of absorbed light in the first 10% of the layer, near to the ITO is 10 times the light intensity absorbed in the far end of the layer. This raises the questions about the accuracy of the reported second-order rate constants and the interpretation of the fast decay of absorption observed during the first 30 μs (Figure 1a). In view of its importance to this as well as other works, we carried a series of computations to study the effect of this kind of inhomogeneity. Simulations of the absorbance vs time profiles were carried out by dividing the 3 μ layer into 10 sublayers, calculating the relative light intensities absorbed by each of the sublayers for overall absorbance of $D = 1.1$. Taking the conditions as employed in Figure 1, with average quantum yield of about 0.15, the I_2^- concentration at each layer is proportional to the square root of the excitation light intensity. Summation of the optical absorbance of the 10 sublayers, and assuming no interlayer diffusion, yields a simulated absorbance vs time profile with very good linear dependency of 1/D vs time. The second-order rate constant $k_9 = 2.33 \times 10^5$ M^{-1} s^{-1} is calculated from the slope for 100−1000 μs. This value is only 3.5% higher than the value $k_9 = 2.25 \times 10^5$ M^{-1} s^{-1} used to create the time profiles in each of the sublayers. A similar calculation for the first 100 μs yields 2.5×10^5 M^{-1} s^{-1}, a value 11% higher than the one in homogeneous conditions. No observable deviation, which could account for much higher reaction rate (such as in Figure 1a) is observed. In conclusion: the inhomogeneity across the layer under our conditions has a marginal effect on the kinetic results.

Diffusion of I_2^- and e^-_{TiO2}. In view of the diffusion-controlled nature of reaction 10 in aqueous solution,[40−42] the relatively low value of k_{10} in the TiO_2 layer is attributed to a slow diffusion rate of I_2^-. The diffusion coeff of I_2^- in the TiO_2 layer can be calculated using Smoluchowski's equation:[43] $k_{10} = 4\pi r D_{diff} N/1000$ M^{-1} s^{-1}, where r is the reaction radius and D_{diff} is the diffusion coeff of I_2^-. Taking a reaction radius $r = 0.5$ nm yields an apparent diffusion coeff $D_{diff}(I_2^-) = 3 \times 10^{-10}$ cm^2 s^{-1}. Note that this value, which is almost 5 orders of magnitude lower than $D_{diff}(I_3^-)$, as measured in refs 44 and 45, depends on the porosity and tortuousness of the TiO_2 film. The reported value of $D_{diff}(I_3^-)$ is only little lower than in aqueous solution ($D_{diff} = 1.6 \times 10^{-5}$ cm^2 s^{-1}), which is comparable to $D_{diff} = 2 \times 10^{-5}$ cm^2 s^{-1} for I^- ions.[46] The remarkable difference in diffusion rates may be attributed in part to the higher TiO_2 particle size used in the previous works. Thus, under our conditions, ion migration in the solution filling the space between nanocrystallites is hindered. The very high concentration of Na^+ and I^- ions (7 M) and their ion pairs further inhibits I_2^- diffusion by increasing viscosity. Apparently, migration of I_2^- by charge transfer, e.g., $(I-I)^- \cdots I^- \rightarrow {}^-I \cdots (I-I)^-$ is not important.

In relatively dilute solutions, the diffusion of negatively charged species can generate potential differences inside the solution phase and induce migration of other ionic species thus affecting the diffusion rate. This is not likely to be the case in the present system (7 M NaI), where the average distance between two I^- or Na^+ ions is only 0.5−0.6 nm, minimizing any charge effect by I_2^-.

The driving force for reaction 9 is the difference between $E^\circ(I_2^-/2I^-) = 1.03$ V[47] and $E^\circ(e^-_{TiO2}/TiO_2) = -0.12 - 0.059$pH.[48] At pH 2.5, this difference is 1.3 V, compared to a driving force of 1 eV for reaction 10. Thus, reaction 9 may also be diffusion-controlled, particularly if the diffusion rates of the reactants are slow compared to homogeneous solutions. In this case $k_9 = 4\pi r D_{AB} N/1000$ M^{-1} s^{-1}, where D_{AB} is the respective sum of diffusion coeffs of the reactants I_2^- and e^-_{TiO2}. The value of r is not known because of the uncertainty concerning the contribution of e^-_{TiO2}. This may range from ~0.2 nm, if e^-_{TiO2} is completely localized, up to ~2 nm, the radius of a TiO_2 nanocrystallite, in the case that diffusion within the same nanocrystallite is very fast, compared to inter-crystallite migration. Using $r = r(I_2^-) + r(e^-_{TiO2}) = 0.5$ nm yields the sum of diffusion coeffs $D_{I2^-} + D_{e^-TiO2} = 5 \times 10^{-10}$ cm^2 s^{-1}, a value close to the diffusion coeff of I_2^-, so that the possibility that

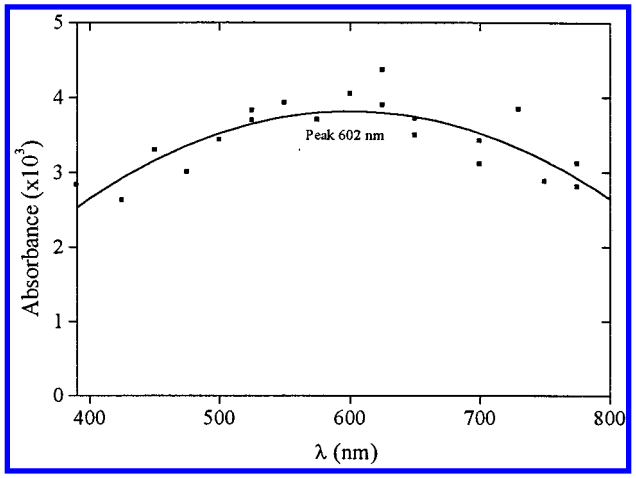

Figure 2. Spectrum of e^-_{TiO2}. Layer immersed in water (no iodide added), pH 2.4 ($HClO_4$). Spectrum obtained 0.5 μs after the laser pulse.

reaction 9 is controlled solely by the diffusion of I_2^- cannot be ruled out. Note that if the reaction radius is higher than assumed above, the resulting value of $D_{I2}- + D_{e\text{-}TiO2}$ is even smaller.

The faster decay in the first 30 μs is attributed to the higher probability of an I_2^- to react with its original electron partner. The time range where this deviation is observed reflects the time, which is required for e^-_{TiO2} and I_2^- to "forget" their original partners, so that reaction 9 becomes homogeneous. With the above calculated diffusion coeff for I_2^-, it is expected to migrate a distance of 1−1.5 nm within 30 μs. The separation distance between the original partners may be higher if the diffusion rate of e^-_{TiO2} is also considered. This distance may be sufficient to separate the original I_2^-/electron pair by a TiO_2 nanocrystallite, decreasing considerably the probability of reaction between the original partners.

Although the present results do not enable an accurate determination of $D_{e\text{-}TiO2}$, the proposed upper limit of the diffusion rate of e^-_{TiO2} is several orders of magnitude lower than reported previously[44,45,49,50] for TiO_2 layer composed of relatively larger nanocrystallites. One possible reason is trapping of the electron at the interparticle boundaries, which are more abundant when small TiO_2 nanocrystallites are concerned. In steady state studies with sufficiently high light intensities, the traps are filled up, and only the faster excess electrons are followed. Indeed, the migration rate of the electron has been found to depend on the electron charge density, with a limiting value reached at one electron per nanocrystallite.[51] Under our conditions, the charge density is under this limit. An activation barrier to diffusion of conduction band electrons in the small particle system is also possible because of particle size distribution, as the electrons are more stable at the larger nanocrystallites.

The spectrum presented in Figure 2 does not enable unequivocal assignment of e^-_{TiO2} to conduction band or trapped electrons. The spectrum induced by the laser pulse in the absence of I^-, peaking at 600 nm, resembles the electron spectrum observed in colloid Q-particles in solution,[25] and differs significantly from the spectrum of electrochemically induced trapped electrons in bulk TiO_2 layer. In the latter case, the absorption increases steadily toward the UV, showing no peak.[23] The peak observed in colloid solutions of the Q-particles,[25] in contrast to conduction band electrons in bulk TiO_2 and in large TiO_2 nanocrystallites, which show no peak, was attributed to quantum effect on the absorption of conduction band electrons. However, localized electrons at surface defects may also account for the observation of a peak.[18] Whatever the exact nature of e^-_{TiO2}, the observation of only one second-order decay process representing reaction 9 suggests that only one kind of electrons is involved.

Comparison between the 390 and 575 nm Decays. The decay at 390 nm, where light is absorbed predominantly by I_2^-, is negligible during the first 50−200 ns. On the other hand, a considerable decay of absorbance takes place at 575 nm, attributed mainly to e^-_{TiO2} (Figure 3). These results are in agreement with earlier work,[24] suggesting that conduction band electrons, produced upon laser photolysis, decay in the ns time range to lower energy states. These lower states may be within or outside the conduction band.

Comparison between the kinetic parameters derived from the time profiles at 390 nm (as shown in Figure 1) and 575 nm (absorption predominantly due to e^-_{TiO2}) was carried out. Figure 4 shows the absorbance vs time profile at 575 nm. Very good agreement between the computed and the experimental profiles is obtained using $k_9 = 2.3 \times 10^5$, $k_{10} = 1.05 \times 10^5$, and $k_{11} = 1.65 \times 10^3$ M^{-1} s^{-1}, $\epsilon^{575}(e^-_{TiO2}) = 2000$, $\epsilon^{575}(I_2^-) = 280$, and $\epsilon^{575}(I_3^-) = 160$ M^{-1} cm^{-1}, the latter was measured in aqueous 7 M NaI (this work). These rate constants agree well with those derived from the I_2^- decay (390 nm profiles in Figure 1). The simulated 575 nm time profiles are not very sensitive to the value of $\epsilon^{575}(e^-_{TiO2})$. The extinction coeff of $e^-_{TiO2} = 2000$ is higher than the published value of 1200 M^{-1} cm^{-1} reported for colloid solutions.[9,25] However, reasonable fit can also be obtained choosing $\epsilon^{575}(e^-_{TiO2})$ in the range 1000−2000 M^{-1} cm^{-1} and adjusting the initial concentrations according to the initial absorbance. The computed value of k_9 decreases with decreasing the value chosen for $\epsilon^{575}(e^-_{TiO2})$. At 1000 M^{-1} cm^{-1}, $k_9 = 1.6 \times 10^5$ M^{-1} s^{-1}.

Effect of Pulsing Rate. The kinetics presented in Figure 1d shows a residual absorbance after 1 s, suggesting that a fraction of the I_3^- ions remains unreacted for several seconds. The relatively long lifetime of I_3^- causes an effect of laser pulsing rate on the observed decay profile: at a high laser intensity and a high pulsing rate of more than 10 pulses per min, residual absorption at 390 nm is accumulated by every additional pulse, until a steady absorption is reached after about 30 pulses. Such build up is not observed at a rate of 2 pulses per min. This effect of pulsing rate indicates that the reaction of I_3^- with e^-_{TiO2} requires about 30 s to complete under our conditions, in agreement with the computed value of k_{11} and the proposed kinetic scheme.

Experiments in the Presence of Thiosulfate. Experiments were carried in the presence of thiosulfate in order to rule out complications due to I_3^-. Thiosulfate is known to reduce I_3^- and prevent its accumulation. Because thiosulfate may react also with I_2^-, the effect of added thiosulfate on the time profiles at 390 nm was tested. Addition of up to 0.005 M thiosulfate has no observable effect on the time profiles up to 4 ms, although the decay is enhanced in the range 5−100 ms. Comparison of the decays at 390 and 575 nm in the presence of thiosulfate shows no decay at 390 nm, in contrast to a pronounced decay during the first 50 ns at 575 nm. These results are precisely identical with observations in the absence of thiosulfate (Figure 3), confirming that accumulation of I_3^- by the repetitive pulses is not responsible for the apparent contradiction between the decay at 390 and 575 nm.

Comparison to Earlier Results. Fitzmaurice et al.[33] reported that I_2^-, produced upon oxidation of iodide at aqueous TiO_2 colloid decays nearly exclusively according to reaction 9 with $k_9 \approx 3 \times 10^{10}$ M^{-1} s^{-1}, in agreement with the earlier report by Draper and Fox.[29] This value, which assumes homogeneous

distribution of I_2^- in the bulk of the solution, is 5 orders of magnitude higher than the value reported here for the TiO_2 layers, reflecting large differences in the diffusion constants. In the colloid system e^-_{TiO2} is unable to migrate from one nanoparticle to another. Diffusion of the TiO_2 particles is negligible compared to the rate of diffusion of I_2^-, and hence, the rate of the second-order reaction 9 is determined by the rate of diffusion of I_2^- in the bulk ($D \approx 2 \times 10^{-5}$ cm^2 s^{-1}). On the other hand, the diffusion of I_2^- and probably also e^-_{TiO2} in the layer system is relatively very slow. Very small accumulation of static absorption of I_3^-, increasing linearly with the number of laser pulses has been observed in the colloid system. This was taken as evidence that reaction 9 is the nearly exclusive path for the decay of I_2^-,[33] with only 4% contribution of reaction 10. This result is considerably different from ours and does not agree with the known rate constant ($k_{10} \approx 3 \times 10^9$ M^{-1} s^{-1} in aqueous solution),[40-42] which predicts significant formation of I_3^-. The apparent discrepancy can be resolved by assuming that in the colloid system reaction 9 takes place between the e^-_{TiO2} and adsorbed I_2^-, which is at equilibrium with I_2^- in the bulk, while the dismutation of I_2^- takes place in the bulk only. It is further assumed that most I^- ions, which are produced by reaction 10 in the colloid system, subsequently oxidize the electrons, but some I^- ions migrate to the bulk and escape this reaction. These ions account for the reported residual absorption in the colloid system. In such case, the residual absorption is expected to depend on competition between reaction 11 and on the rate of desorption of I^- and on the Langmuir adsorption coeff of I_2^-. If most I_3^- ions in the bulk avoid recombination with electrons, the buildup of I_3^- absorption is expected to be linear with the number of pulses, as indeed observed in the colloid systems. On the other hand, in the layer system, desorption of I_2^- and I_3^- is supposedly fast and complete because of quick exchange with I^- ions, which are present at very high concentration.

The driving force for reaction 9, 1.3 V under the conditions of this work, is much larger than the driving force for reaction 11, which is only 0.2 V. Consequently, reaction 11 is considerably slower than reaction 9.

In a photoelectrochemical cell based on I^-/I_3^- charge carrier, a typical I_3^- concentration is $\approx$ 0.01 M. If the value of k_{11} reported in the present manuscript applies to the photoelectrochemical systems, reaction 11 is expected almost completely to suppress the photocurrent. However, some of these cells show very high photocurrent yields. Note that in the photoelectrochemical cell system, an overall two-electron reduction takes place. This reaction has been reported to proceed via I_2^- (in equilibrium with I_3^-), with rate proportional to the second power of I_3^- [45-49] and charge density.[49] Reduction mechanism of I_3^- in the photoelectrochemical cell may involve the consecutive reaction 9 and 11, although an uncommon simultaneous two-electron-transfer cannot be ruled out. The results of the present study indicate the reduction of I_3^- by e^-_{TiO2} at the surface of bare TiO_2 nanocrystallite layer is sufficiently fast to prevent a significant photocurrent. Alternative reduction mechanism, such as simul-